

Project no.:

608608

Project acronym:

MiReCOL

Project title:

Mitigation and remediation of leakage from geological storage

Collaborative Project

Start date of project: 2014-03-01

Duration: 3 years

D4.2

The impact of hysteresis effects on brine/CO₂ relative permeability and CO₂ recovery as remediation measure

Status: definitive

Organisation name of lead contractor for this deliverable:

TNO

Project co-funded by the European Commission within the Seventh Framework Programme		
Dissemination Level		
PU	Public	X
PP	Restricted to other programme participants (including the Commission Services)	
RE	Restricted to a group specified by the consortium (including the Commission Services)	
CO	Confidential , only for members of the consortium (including the Commission Services)	

Deliverable number:	D4.2
Deliverable name:	The impact of hysteresis effects on brine/CO ₂ relative permeability and CO ₂ recovery as remediation measure
Work package:	WP4: Reservoir pressure management as CO ₂ migration and remediation measure
Lead contractor:	GFZ

Status of deliverable		
Action	By	Date
Submitted (Author(s))	Cor Hofstee	2 July 2015
Verified (WP-leader)	Conny Schmidt-Hattenberger Conny Schmidt-Hattenberger (updated version)	24 August 2015 23 January 2017
Approved (SP-leader)	Axel Liebscher	28 August 2015
Approved (Coordinator)	Holger Cremer	23 January 2017

Author(s)		
Name	Organisation	E-mail
Cor Hofstee	TNO	Cor.hofstee@tno.nl

Public abstract
<p>This report is part of the research project MiReCOL (Mitigation and Remediation of CO₂ leakage) funded by the EU FP7 program¹. Research activities aim at developing a handbook of corrective measures that can be considered in the event of undesired migration of CO₂ in the deep subsurface reservoirs. MiReCOL results support CO₂ storage project operators in assessing the value of specific corrective measures if the CO₂ in the storage reservoir does not behave as expected. MiReCOL focuses on corrective measures that can be taken while the CO₂ is in the deep subsurface.</p> <p>This deliverable reports on the impact of hysteretic relative permeability on intended or unintended venting of the aquifer. Furthermore, the impact of hysteresis is compared with the role of diversion of the CO₂ by the injection of brine. To avoid increasing the definition of the storage complex, the injected brine was produced from the same compartment.</p> <p>Dynamic flow simulations were applied to selected reservoir models to test the effects of hysteresis on CO₂ recovery and reservoir pressure management. A limited sensitivity study was conducted to determine the impact of duration of redistribution, permeability, pore volume and amount injected on the venting process. In addition it was attempted to lower the CO₂ emissions during a venting procedure, by injection of water into the CO₂ zone.</p>

¹ More information on the MiReCOL project can be found at www.mirecol-co2.eu.

Public introduction (*)

CO₂ capture and storage (CCS) has the potential to reduce significantly the carbon emission that follows from the use of fossil fuels in power production and industry. Integrated demo-scale projects are currently being developed to demonstrate the feasibility of CCS and the first such projects are expected to start operating in Europe under the Storage Directive in the period 2015 – 2020. For the license applications of these projects a corrective measures plan is mandatory, describing the measures to be taken in the unlikely event of CO₂ leakage. This project will support the creation of such corrective measures plans and help to build confidence in the safety of deep subsurface CO₂ storage, by laying out a toolbox of techniques available to mitigate and/or remediate undesired migration or leakage of CO₂. The project is particularly aimed at (new) operators and relevant authorities.

In this report the impact of hysteresis on the venting process is investigated. The impact of hysteresis is compared with diversion of the CO₂ by the injection of brine. To avoid reservoir increases, the injected brine was produced from the same compartment.

Like all other Work packages of MiReCOL, the results of this work will contribute to later activities that will assess the effectiveness and consequences of all leakage mitigation measures, leading to the production of a Corrective Measures Handbook.

TABLE OF CONTENTS

	Page
1 NUMERICAL MODELLING OF A SALINE DEEP AQUIFER	2
2 MATERIAL AND METHODS	3
3 THE IMPACT OF HYSTERESIS ON THE LONG-TERM EXTENT OF THE MIGRATION.	6
4 WATER INJECTION COMBINED WITH WATER PRODUCTION AT A LARGE DISTANCE.	11
5 CONCLUSIONS	21
6 REFERENCES	22
APPENDIX 1	23

1 NUMERICAL MODELLING OF A SALINE DEEP AQUIFER

During injection of CO₂ in a storage compartment of a gas field, the ambient fluids in the reservoir are displaced. In the case of the mature gas field P18-4, for example, the injection CO₂ enters the available pore space involving displacement and gradually mixes with the remaining natural gas molecules. In this situation the water phase is not or hardly displaced. During the event of venting, the re-production should therefore not be subject to hysteresis. In the case of an aquifer, the CO₂ is injected in a pore space, which is occupied by the brine phase. This means that the wetting fluid (= brine) is displaced (so-called drainage process). The space occupied by the injected CO₂ is created by the increase of the reservoir pressure, which leads to compression of the brine. Reversal of the flow during the event of venting (opening injector) would result in hysteresis and relative permeability-saturation curves, which are a function of the displacement history (reversal points, entrapment etc.) (Corey, 2004). Although hysteretic characteristic curves are routinely employed by the petroleum industry, researchers in other fields, such as those of geothermal energy systems and CO₂ storage, tend to assume non-hysteretic conditions (Doughty, 2007). Several expressions have been derived for describing hysteretic relationships. Examples are Lenhard and Parker (1987) and Parker and Lenhard (1987). Oak (1990), however, mentioned that many data sets (used in CCS studies), are at best limited to just a couple of measured saturation history cases. Recent work by Benson et al. (2015) indicated that the situation has hardly improved in the last 25 years. Besides during venting, reversal of displacement also occurs when brine re-imbibes (displacement of non-wetting (= CO₂) by wetting fluid) into areas, vacated by the CO₂ during its redistribution within the aquifer. The entrapment, associated with hysteresis, also increases the interfacial area between the CO₂ and the brine. This leads to more rapid dissolution.

Venting as a remediation technique was studied in a simulations study by Esposito and Benson (2012). They considered the removal of as much as possible gaseous CO₂ from shallow (100 m deep) aquifers. These aquifers received various quantities (up to 50000 ton) of CO₂ through a faulty well. Depending on the shape of the CO₂ plume, horizontal or vertical wells were used. Injection of water was also considered. While this study demonstrated that CO₂ removal is possible, the effectivity of various remediation approaches was found to vary depending on the quantity of CO₂, and the permeability distribution in the aquifer. For this project, a static geological model of an actual unnamed aquifer was selected. Furthermore, venting of CO₂ works also as potential corrective measure to reduce the overpressure, typically around 10-20 % over the initial pressure, as shown by Neele et al., 2011.

After a description of the simulation approach, we first demonstrate the importance of including hysteretic properties in the simulation of venting procedures (Chapter 3). This is done by comparing the results of non-hysteretic prediction with hysteretic modelling. This is followed by a sensitivity analysis of the venting procedures, where parameters, such as permeability, injection rates and the pore volume will be varied. In Chapter 4, the hysteresis is further enhanced by the injection of large volumes of water. To avoid increases in the reservoir pressure, this injected brine is produced in the same aquifer. Again a sensitivity analysis is done with various water injection schemes and the cumulative CO₂ injection.

2 MATERIAL AND METHODS

The starting point of the current study was a non-hysteretic reservoir model. The non-hysteretic relative permeability-saturation curves (Figure 1) of the carbon dioxide and the brine were made hysteretic by applying the EHYSTER keyword (Eclipse reservoir simulation software), with an entrapped non-wetting fluid saturation of 0.1. This means that below a minimum CO₂ saturation (0.1 in this case), the gaseous phase is considered to be discontinuous and the relative permeability of the CO₂ phase goes to zero.

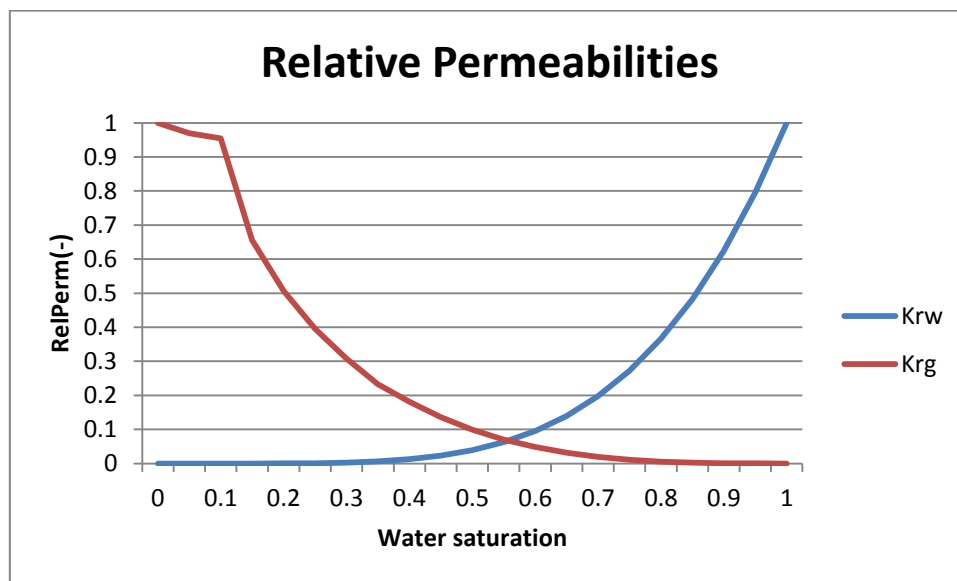


Figure 1. Original non-hysteretic relative permeability values, where the subscript w and g stand for water and brine, respectively.

Prior to further simulation, the aquifer underwent a cumulative injection of $3.2 \cdot 10^{10} \text{ Sm}^3$ (58 Mt), between 2009 and 2018 (Figure 2). The post-injection saturation distribution and reservoir pressure are shown in Figure 3 and Figure 4, respectively.

With this model, a number of simulations were carried out. Back production of CO₂ as predicted by the reservoir model was compared with and without a hysteretic description. A sensitivity analysis was carried out concerning periods between the end of injection, and the actual back production. Further investigations involved 1) The impact of hysteresis on combined water injection and venting mitigation technique (Section 3). 2) Massive water injection was applied in an attempt to immobilize and/or push the CO₂ away from a possible faulty well (Section 4).

Simultaneous water injection and venting was simulated by introducing a separate injector at the location of the CO₂ injector. For these scenario's only hysteretic predictions were made.

It should be noted that the reservoir simulator reports several predictions at selected times only. This means that figures in this report may show steps functions, which in reality should be smooth continuous lines.

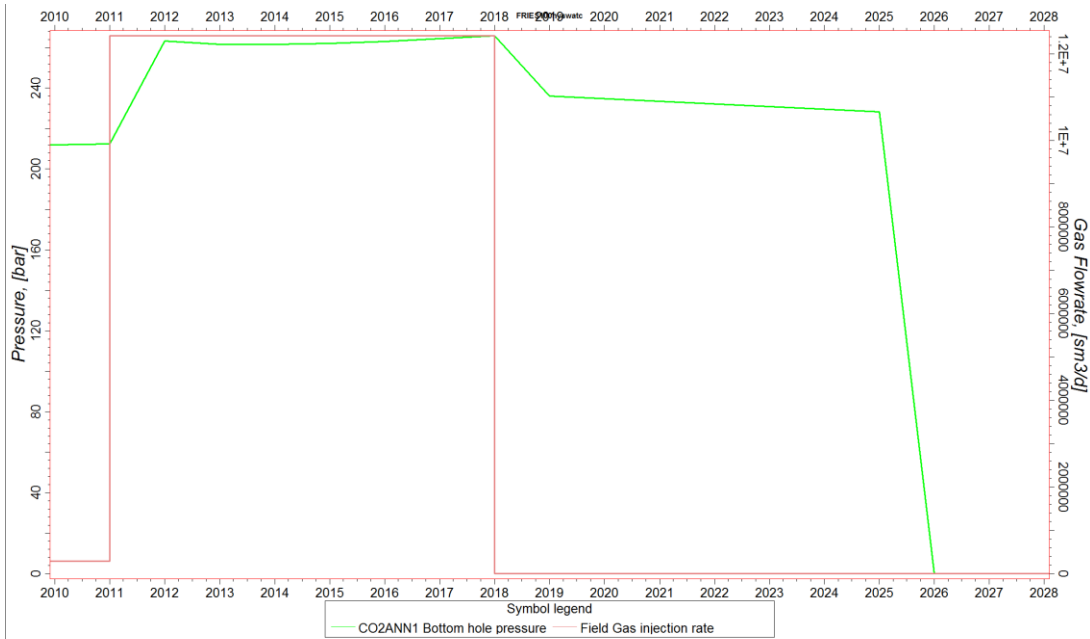


Figure 2. Injection profile (Red) for around 60 Mt CO₂ and bottom hole pressure (BHP) of the injector (green), as used as starting point for all scenarios.

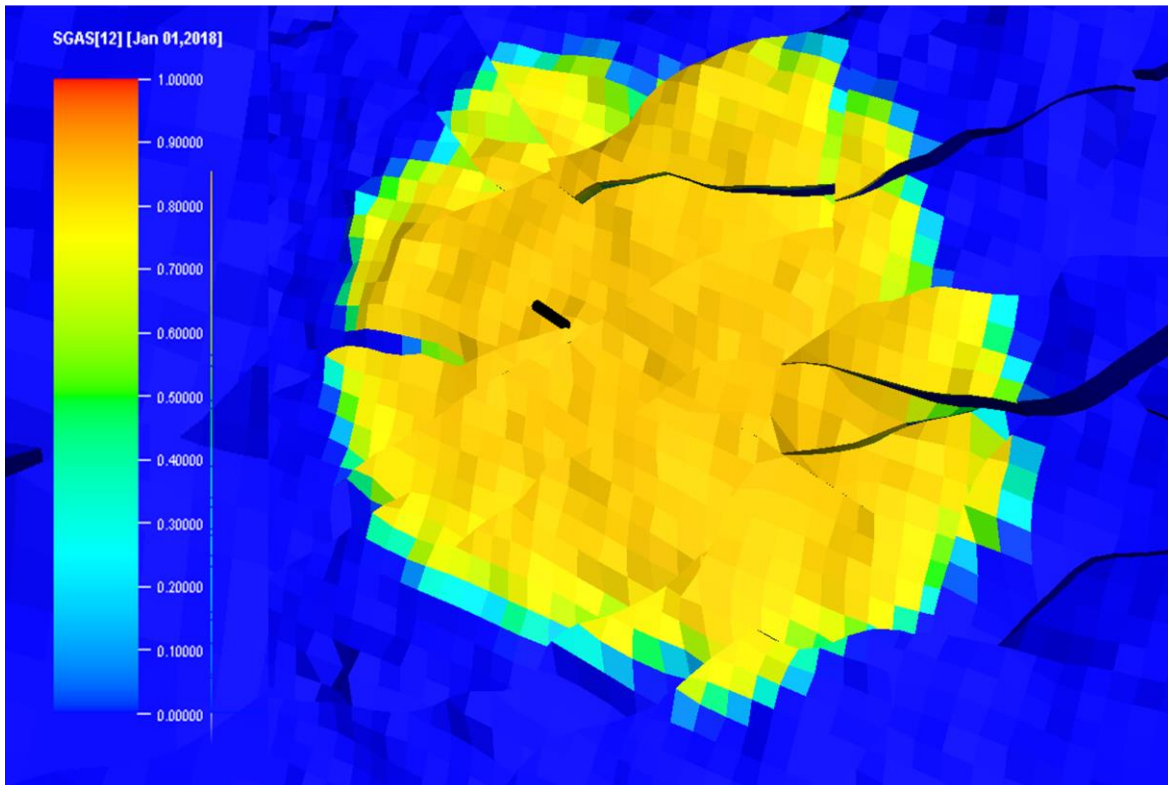


Figure 3. CO₂ saturation distribution around two injectors, at end of injection period. The size of the CO₂ plume is around 6.8 by 4.7 km.

Venting was initiated by changing the injector into a producer and applying a minimum bottom hole pressure (BHP) constraint to that producer. Simultaneous water injection and venting was simulated by introducing a separate injector with the same completion/coordinates of the venting well. This injector was constrained with an injection rate constraint. The earlier studies confirmed that the injection pressure did not exceed the maximum reservoir pressure. Figure 3 shows the impact of the many faults in the area on the migration of the injected CO₂. During the aforementioned feasibility study, each fault in the aquifer was evaluated. Although many of the faults show some connectivity issues, the overall pressure buildup was practically homogeneous, throughout the aquifer (Figure 4). The only exception was the higher pressure near the injector during injection.

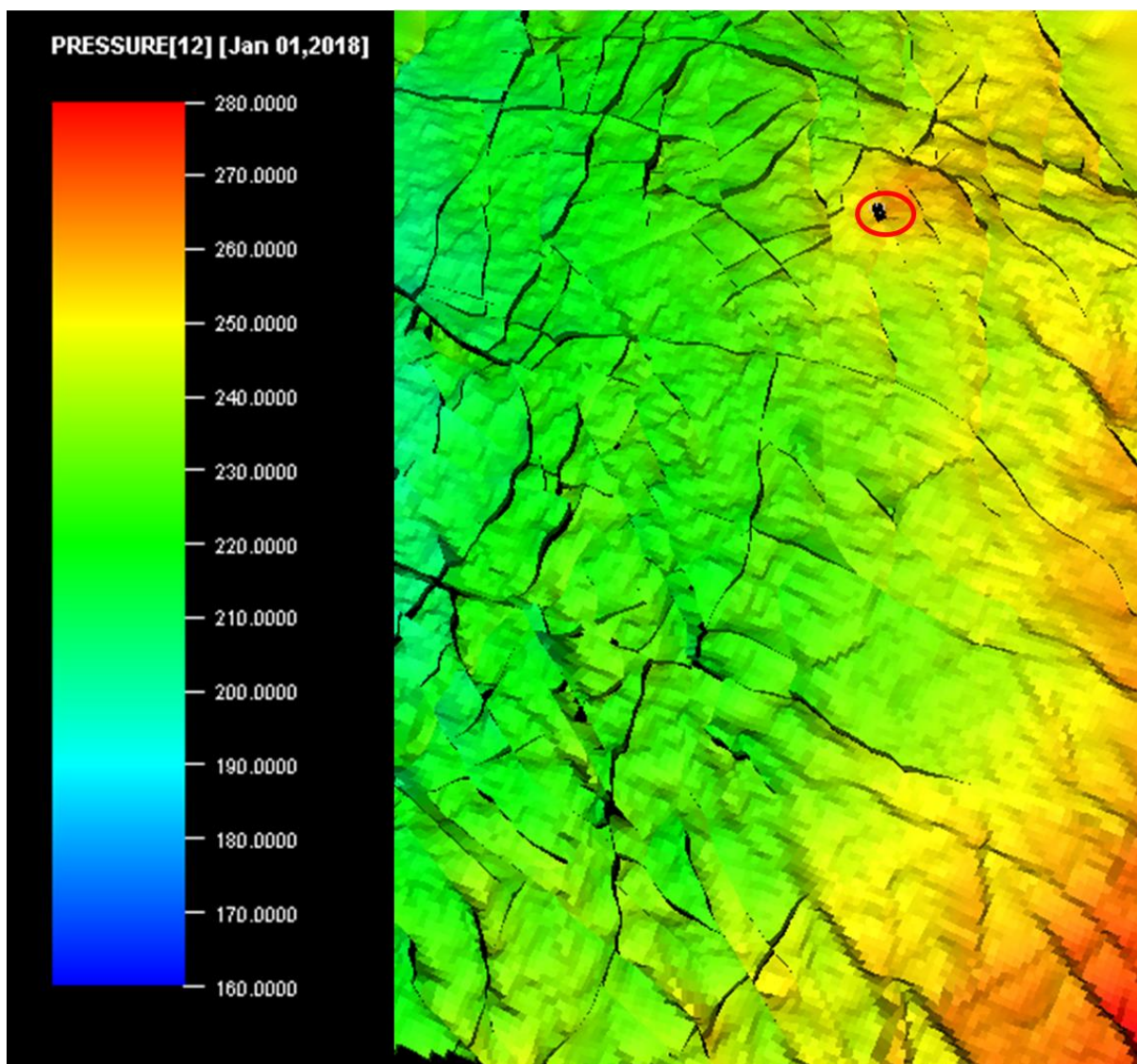


Figure 4. Constant pressure (around 240 bar) distribution at the end of injection, indicating good overall connectivity throughout the reservoir. The red circle indicates the position of the injector.

3 THE IMPACT OF HYSTERESIS ON THE LONG-TERM EXTENT OF THE MIGRATION.

In the following, the role of hysteresis on the venting process will be demonstrated by comparing a hysteretic with a non-hysteretic prediction of several scenarios (Table 1). In addition, the impact of time between the end of injection and the unwanted flow is looked at. This is done by comparing 2190 days (6 years) of redistribution time with 11315 days (31 years), prior to the start of the CO₂ back production procedure.

Table 1. Overview of scenarios looking at the impact of post-injection redistribution time and hysteresis on the emission rates during venting.

Scenario	Redistribution time (years)	Permeability
2a	6	non-hysteretic
2b	6	hysteretic
3a	31	non-hysteretic
3b	31	hysteretic

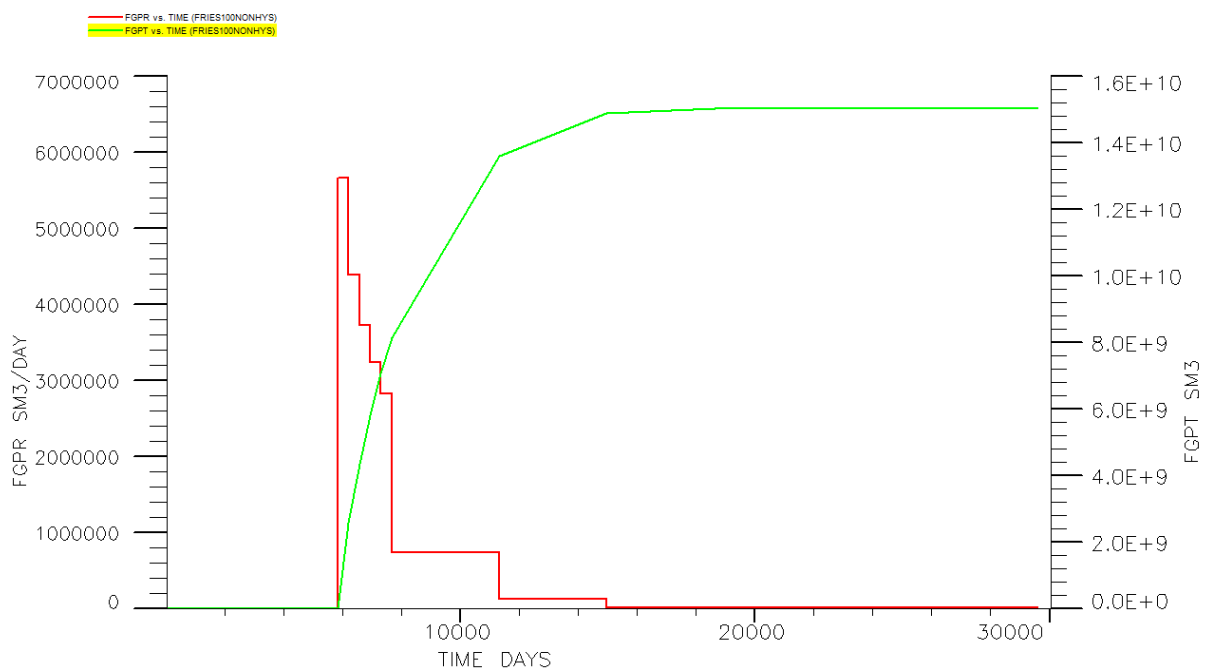


Figure 5. Venting rates (in red) and cumulative emission (in green) as a function of time for the non-hysteretic venting (scenario 2a), 2190 days or 6 years after the end of injection. It should be noted that the number of days on the x-axes include the time of injection.

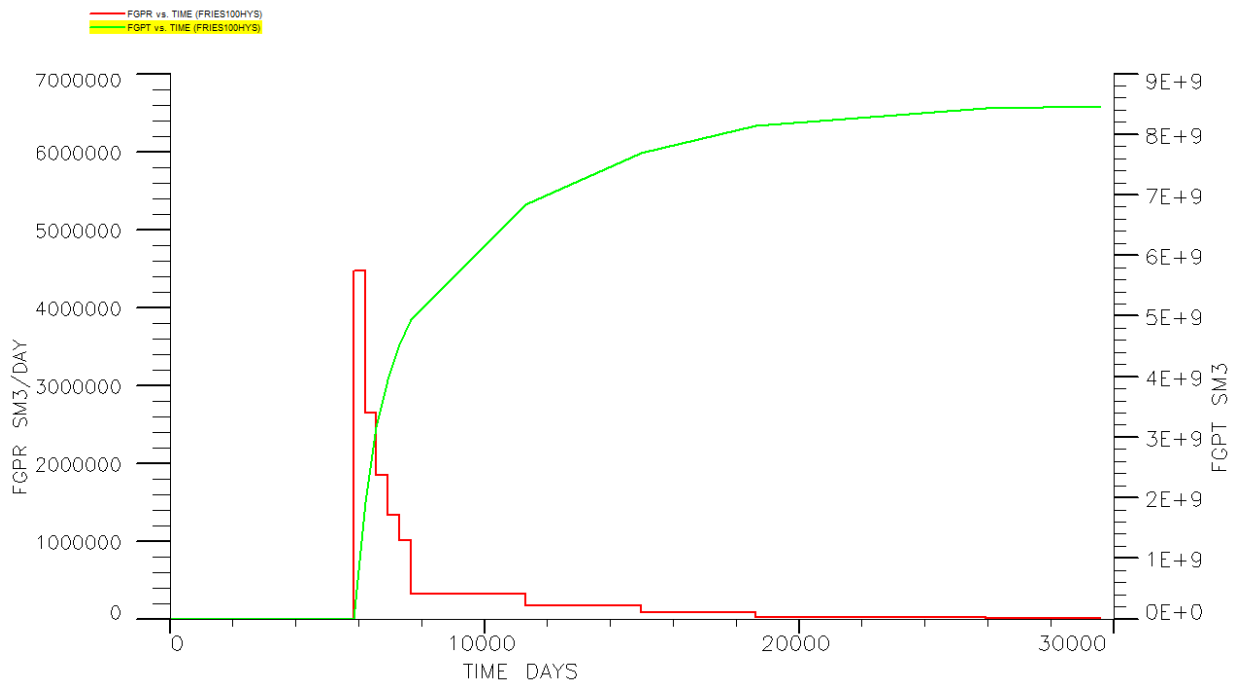


Figure 6. As Figure 5 but with hysteretic relative permeabilities (scenario 2b) for the CO₂ phase.

Figure and Figure show the back production rates as a function of time as predicted by a non-hysteretic and hysteretic model, respectively. The hysteretic case shows both lower initial production rates (4.4 versus 5.6 MSm³/day) and ultimate back production (27 versus 48 % of the injected CO₂ (3.2·10¹⁰ Sm³), lower, than in the non-hysteretic case. This is as expected as hysteresis allows for capillary entrapment of the CO₂ and also the differences (between hysteretic and non-hysteretic cases) in relative permeability at specific saturations.

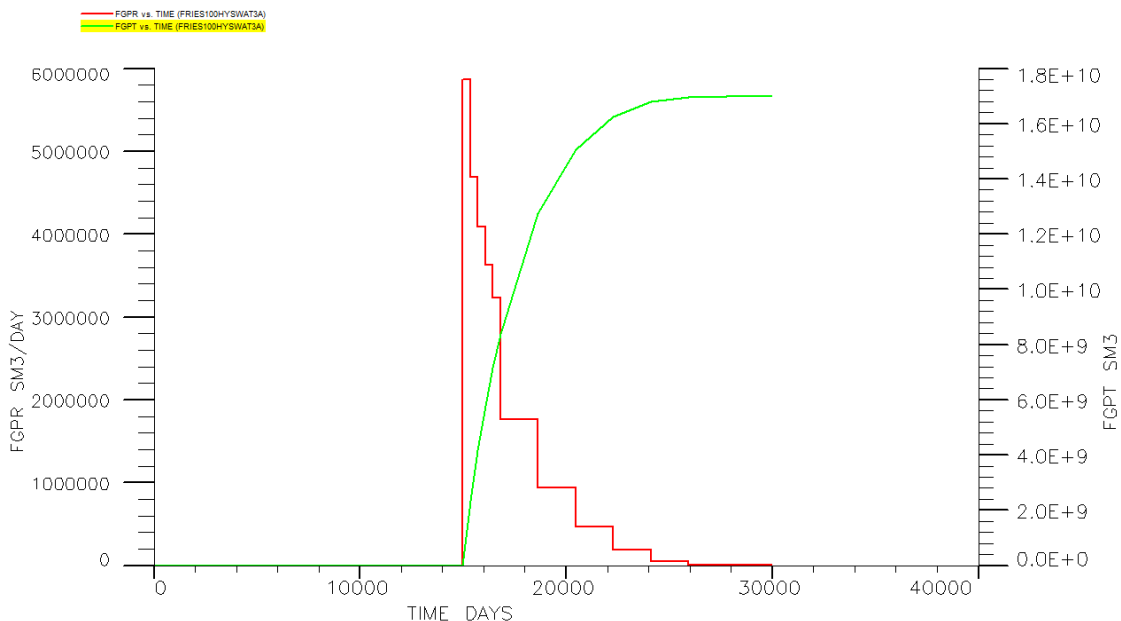


Figure 7. Back production 11315 days, or 31 years, after end of the injection (non-hysteretic simulation).

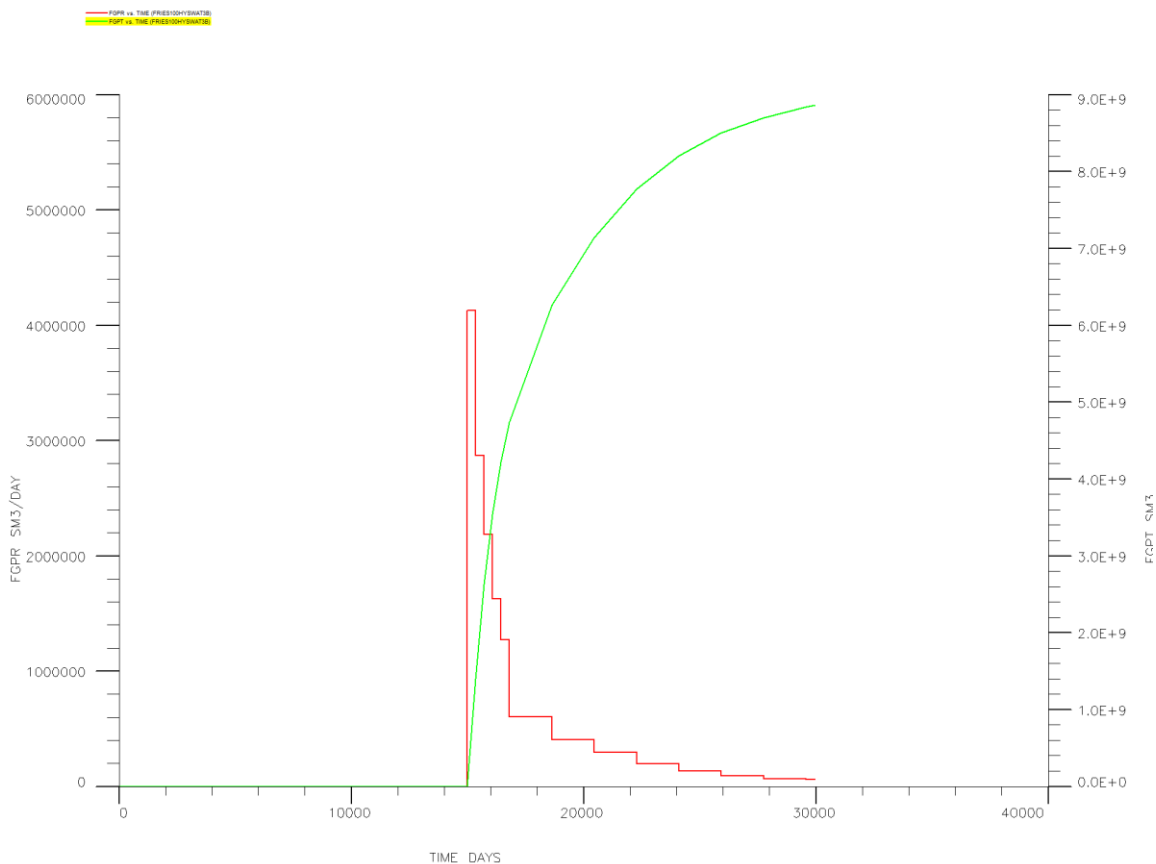


Figure 8. Back production 11315 days, or 31 years, after end of the injection (hysteretic).

Figure and **Error! Reference source not found.** show the venting rates, after the CO₂ was allowed to migrate for 11315 days (31 years) before the start of this venting.

Table 2 reveals that the process of hysteresis has a significant impact on emission rates during venting. As expected, the initial venting rate of the hysteretic case is lower than the corresponding rate for the non-hysteretic scenario, and drops faster with time. Unexpectedly, the hysteresis has a little bit more impact after 6 years of redistribution of the CO₂, then after 31 years. The saturation distribution after the venting during scenario 3b is shown in Figure . The faults in the reservoir are likely to have attributed to the no-uniform gas saturation distribution. It can be concluded that for an accurate prediction of the emission rates during venting, hysteresis should be included in the simulation.

Additional simulations showed that the emission rates increased with reducing the pore-volume (by a factor 2). This can be attributed to the higher saturations near the injector.

Table 2. Overview of the cumulative emission for the various scenarios.

Scenario	Cumulative emission ($\cdot 10^9 \text{ Sm}^3$)	% of total injected CO ₂
2a	15.5	48.0
2b	8.4	26.3
3a	17	53.0
3b	8.8	27.5
Multipv 0.5 compensated elsewhere	10	31
Multipermx 4	12.4	38.7
Multipermx 0.5	12.5	39.1
0.5 injection	2.16	13.1
0.25 injection	$3.4 \cdot 10^{-2}$	0.43
0.125 injection	$7.8 \cdot 10^{-4}$	0.20
0.0625 injection	0	0

In addition, Table 2 shows that the pore volume and permeability adjustment have limited effect on the cumulative emission during venting. These can therefore not be seen as key factors. The percentages of back production reduce with lower amount of CO₂ in the aquifer. This can be attributed to more relative migration (extra space due to lower volume in same aquifer) and also more impact of hysteresis. This also explains why venting experiments in current aquifer storage pilots shows limited emissions. An example is the Frio test, where limited venting rates were reported after a small injection of 1.6 tonnes of CO₂ (Hovorka, 2006). The figures of the 7 last predictions in Table 2 can be found in the Appendix. These cases were run with the hysteretic mode, only.

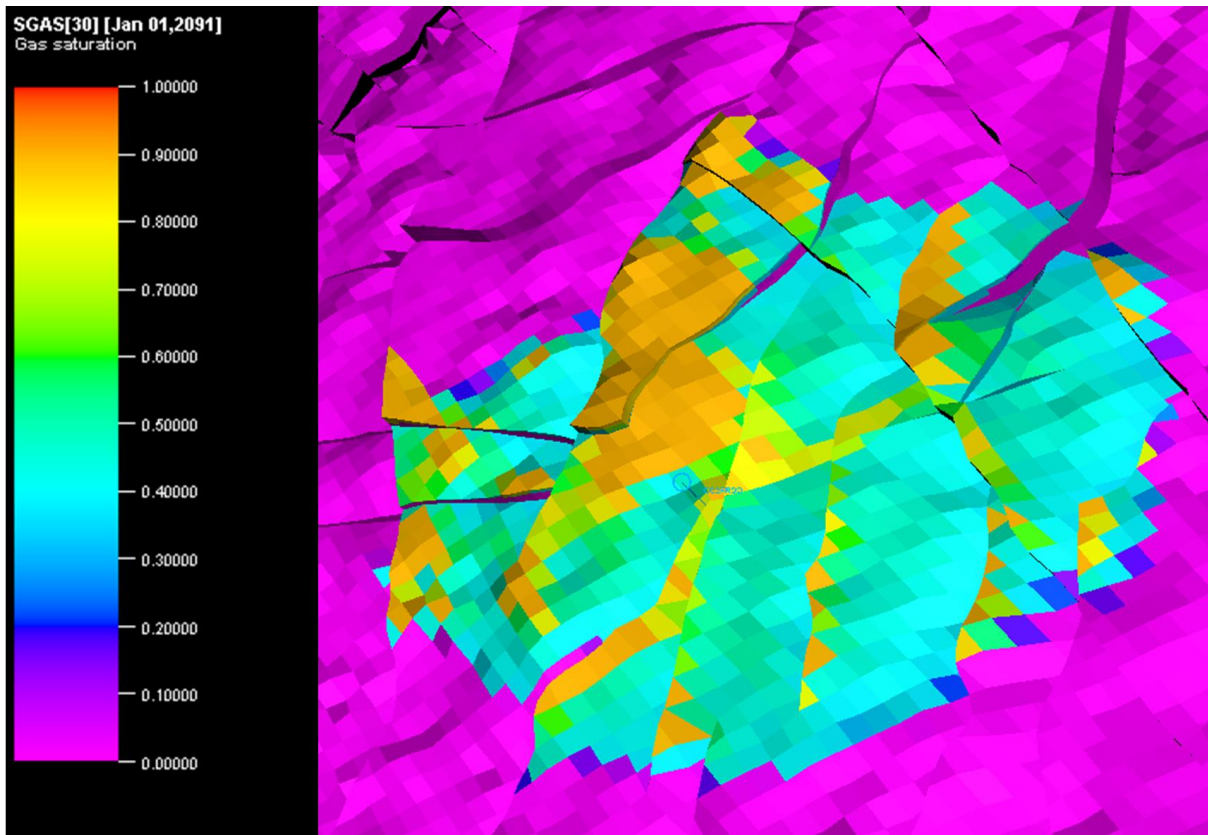


Figure 9. Non uniform CO₂ saturation profile after the venting of CO₂ (scenario 3b).

4 WATER INJECTION COMBINED WITH WATER PRODUCTION AT A LARGE DISTANCE.

In an effort to further enhance hysteresis, in the following simulations, large amounts of water will be injected. By itself this would lead to unwanted increase in the reservoir pressure. To avoid this, a water producer was installed outside the CO₂ plume (Figure 10). The production rate of this producer was set at 77000 Sm³/d for a duration of 13 years. This produced water was re-injected in the injection well. This means that the average reservoir pressure is constant during this operation. After the water production/reinjection was halted, the previously closed injector was opened completely. The 7 years between the end of injection and the start of back production represents the required time for detection of the leakage and also to allow some time for migration of the injected CO₂.

Four scenarios were tested:

- Scenario 4a) 12 years of water injection, starting 2555 days or 7 years after the end of CO₂ injection, followed by continued CO₂ back production.
- Scenario 4b) Continuous simultaneous venting and water injection in at same injector location, starting 7 years after the end of the injection scheme. This scenario was repeated 3 times (scenario f, g, and h) with increasing reduced amounts of stored CO₂.
- Scenario 4c) Simultaneous water injection/production period, starting 2190 days or 7 years after the end of the CO₂ injection, and continuing for a total of 4745 days or 13 years. Continued venting of CO₂ (without water injection) starts 1825 days after start water injection.
- Scenario 4d) as for 4c but with a longer period (7665 days, or 21 years) of simultaneous production and injection of water.
- Examples of the injection/production procedures of scenario 4a and 4b are shown in Figure and Figure , respectively.

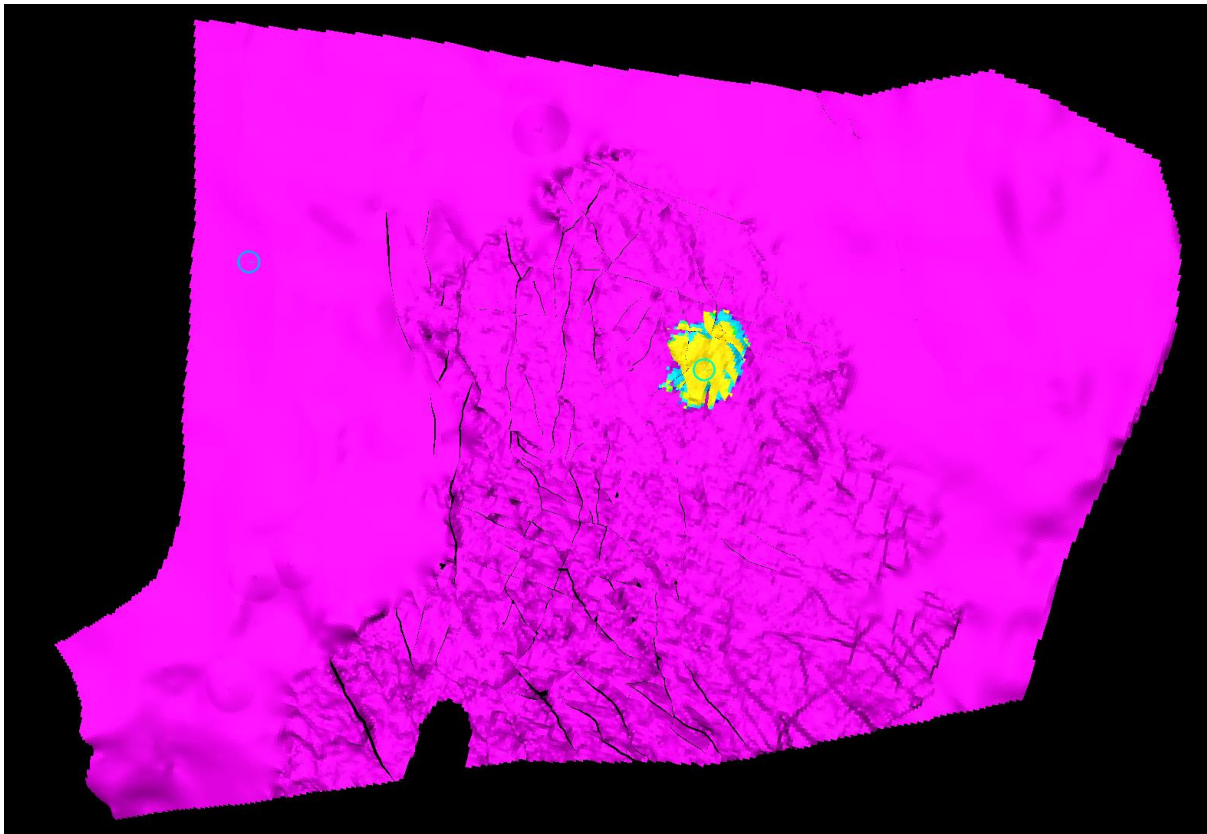


Figure 10. Position of **water** production well (to the left, at a distance of 33600 m), relative to that of the injection/venting wells (to the right) as shown in a gas saturation plot of the aquifer.

Figure shows that venting of CO₂ cannot be prevented by this approach. This means that the anticipated hysteresis (entrapment) has not lead to complete immobilization of the CO₂ phase, Figure indicates indeed gas saturation levels in the range of 0.4 to 0.5. This is above the maximum entrapment saturation of 0.1. The CO₂ is still mobile.

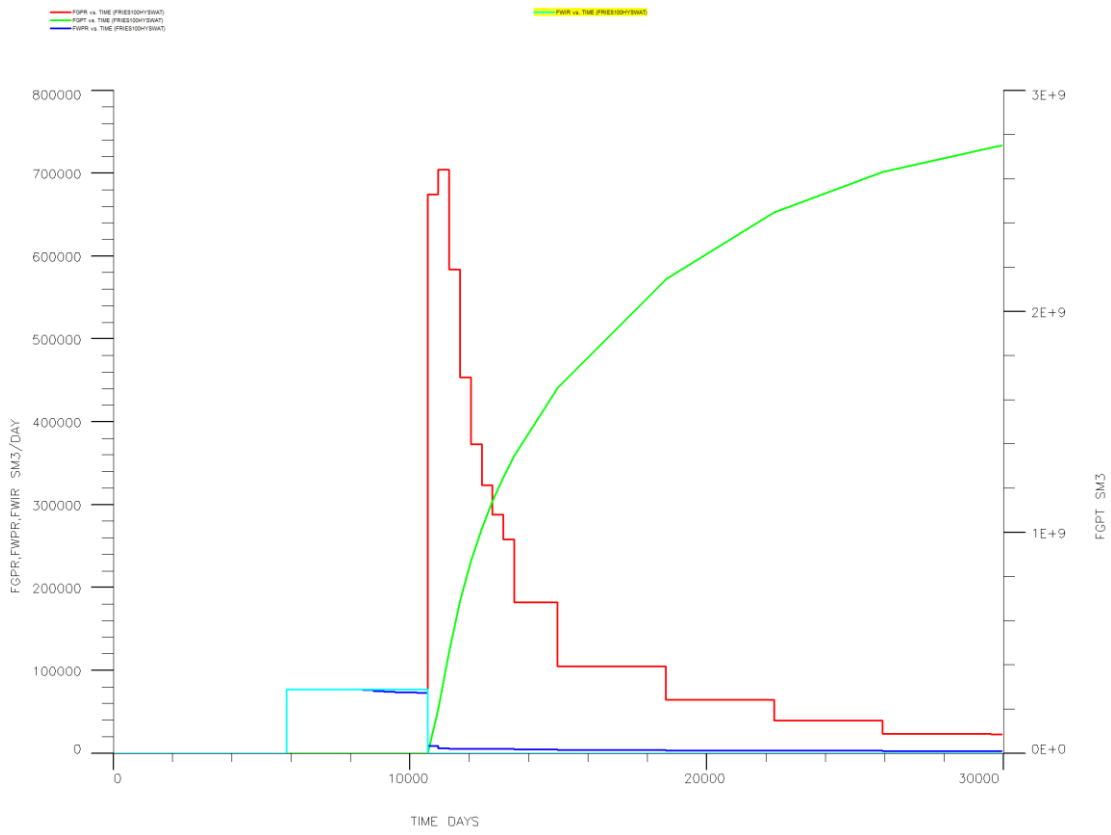


Figure 11. The produced/injected water rates (dark and light blue, respectively), the vented CO₂ rate (red) and cumulative amount of reproduced CO₂ (green) of scenario 4a.

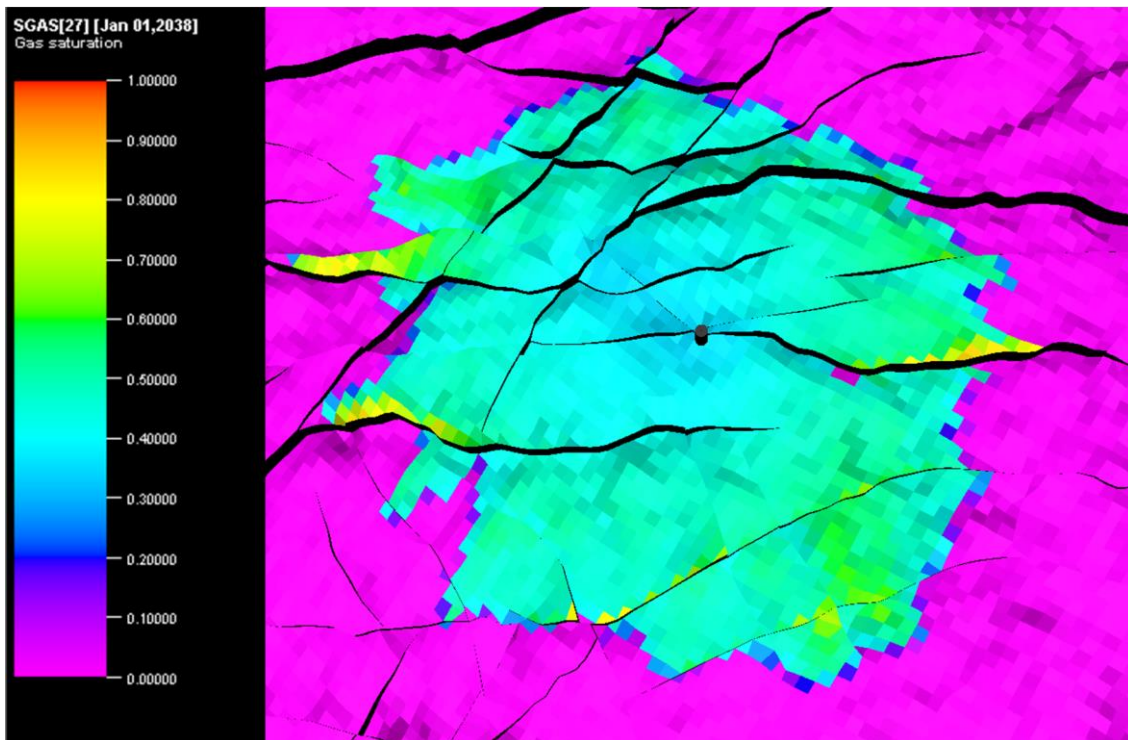


Figure 12. Final CO₂ saturation distribution (size around 8.2 by 7.2 km) after water injection (scenario 4a). The green colour indicates saturation values around 0.4 to 0.5. More yellow stands for higher saturations, with red indicating a saturation of 1.0.

Scenario 4a assumes that one has the luxury of having prior knowledge on a future issue with the integrity of the storage capacity leak. The following scenario starts the water injection at the time of the first emissions of CO₂. This second set of simulation was conducted with hysteretic relative permeability, only.

Figure shows the CO₂ back production rates as a function of time after the venting was started at the start of the water production and re-injection. Unfortunately, the simultaneous venting and injection of water again lead to some emission of CO₂. Figure shows areas with high CO₂ saturation along areas which are more water rich. The amount of emission, however, is much lower than for scenario 4a.

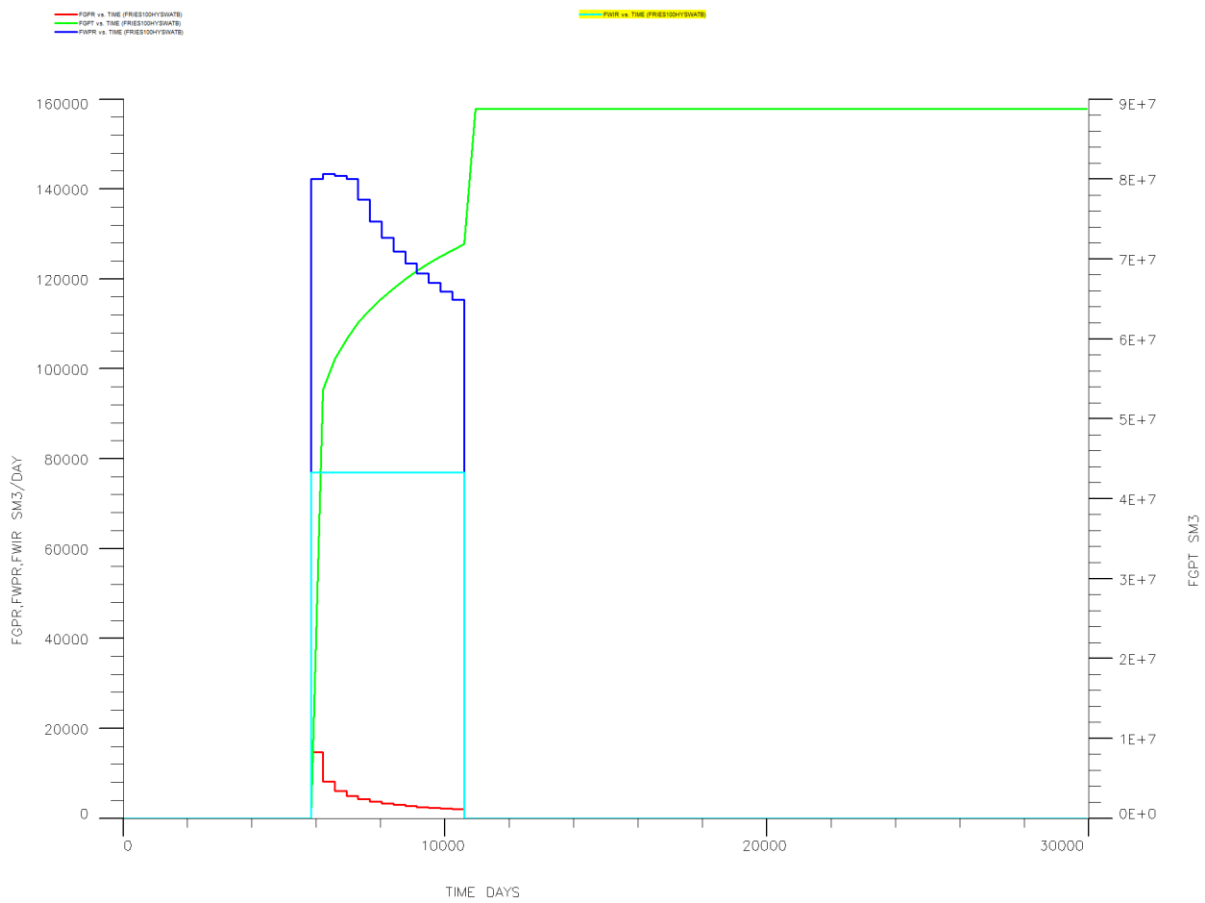


Figure 13. Continuous simultaneous venting (red is rate and green is cumulative) and water injection/production (light and dark blue, respectively) in same injection location, starting 7 years after the end of the injection scheme (scenario 4b).

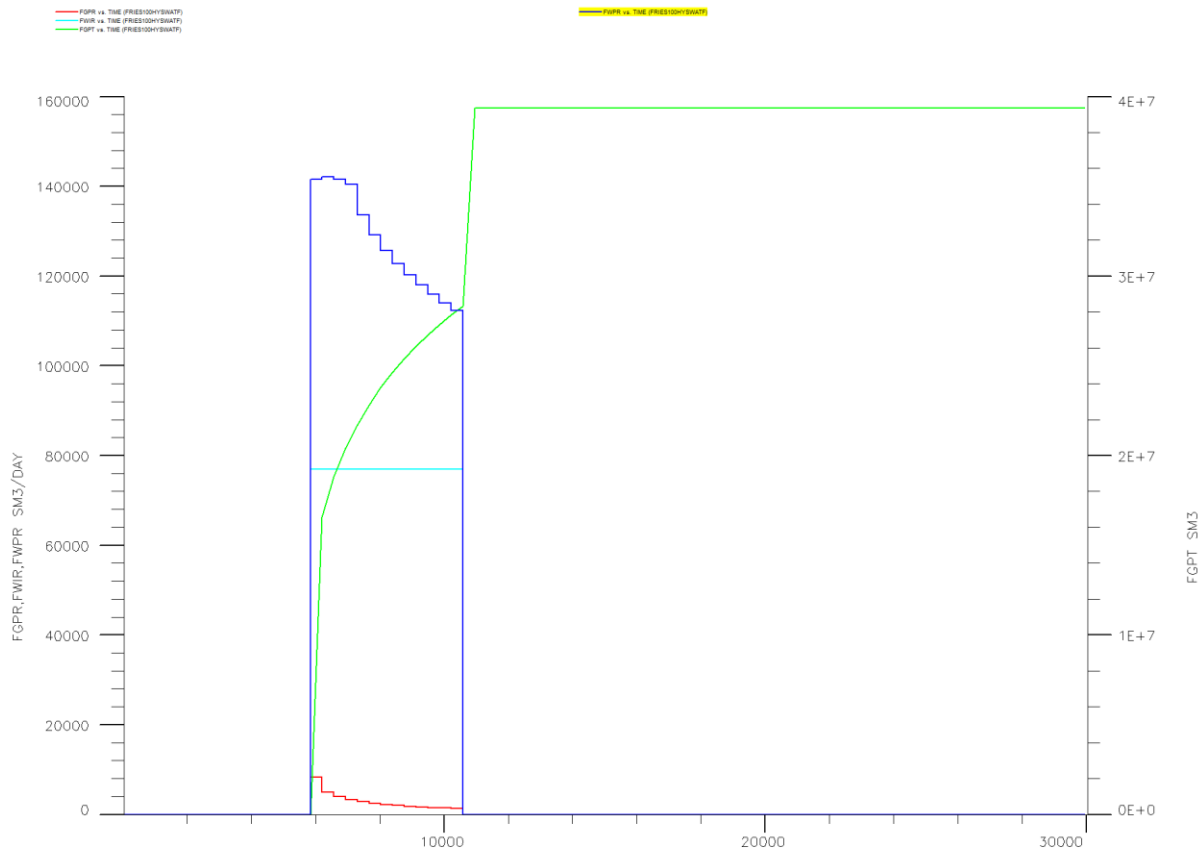


Figure 14. As scenario 4b, but with less CO₂ injection ($2.26 \cdot 10^{10} \text{ Sm}^3$).

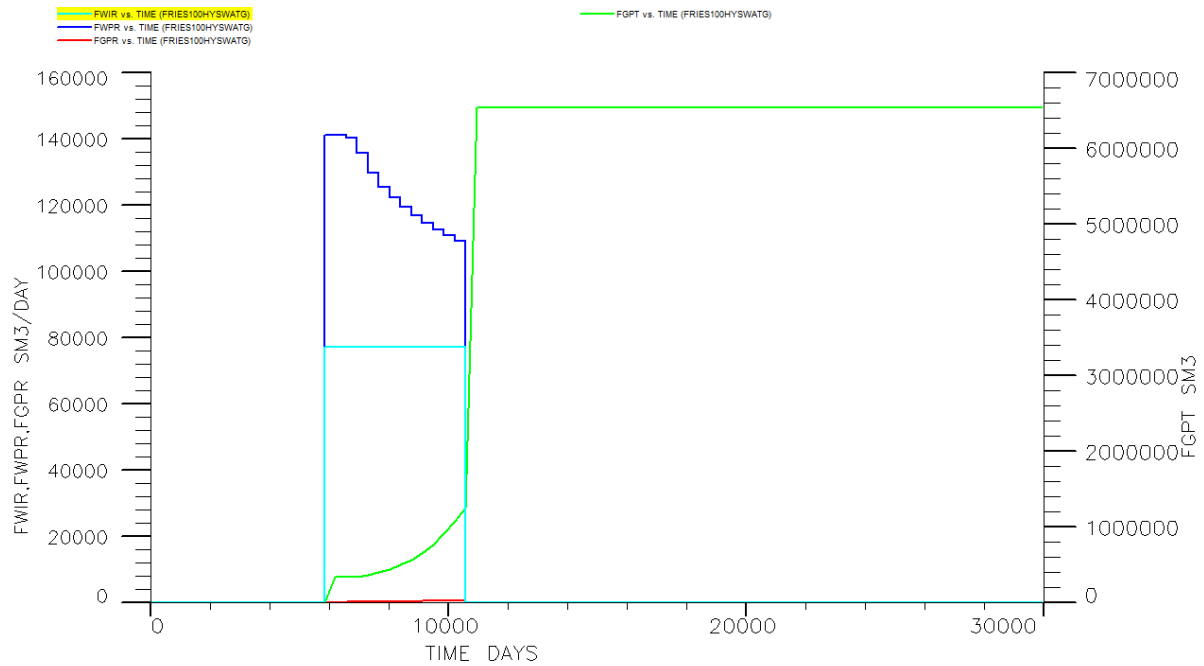


Figure 15. As scenario 4b, but with less CO₂ injection ($1.15 \cdot 10^{10} \text{ Sm}^3$).

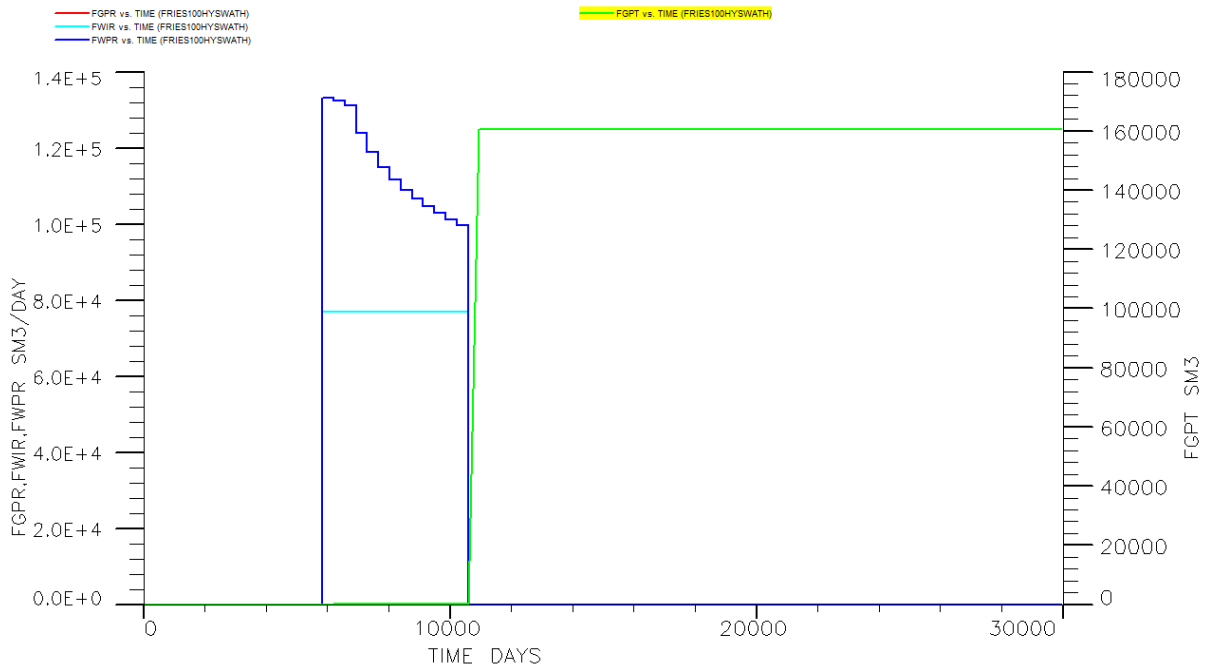


Figure 16. As scenario 4B, but with less CO₂ injection ($9.8 \cdot 10^8 \text{ Sm}^3$)

Scenario 4b was repeated several times with reducing amount of stored CO₂. Figure , Figure and Figure show the emission of CO₂ decrease with the amount of CO₂, which is stored. In Figure , the water injection almost complexly eliminates the emissions.

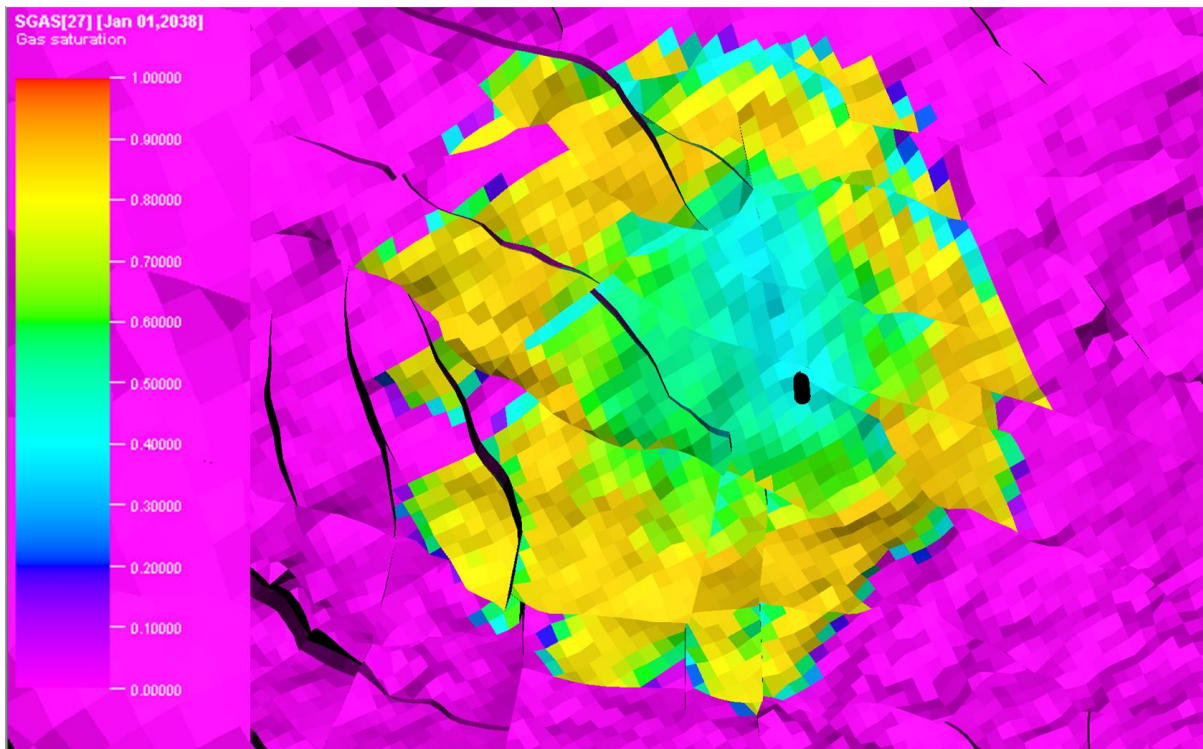


Figure 17. High CO₂ saturation (0.8-0.9) (in red) and lower (0.4-0.5) CO₂ saturation (green/yellow) distribution, after simultaneous venting and massive water injection (scenario 4b).

In simulations of scenario 4c, the water recirculation was continued for just 6 years after the CO₂ back production started. This limited period of the water injection clearly lead to a second peak in venting rates (Figure).

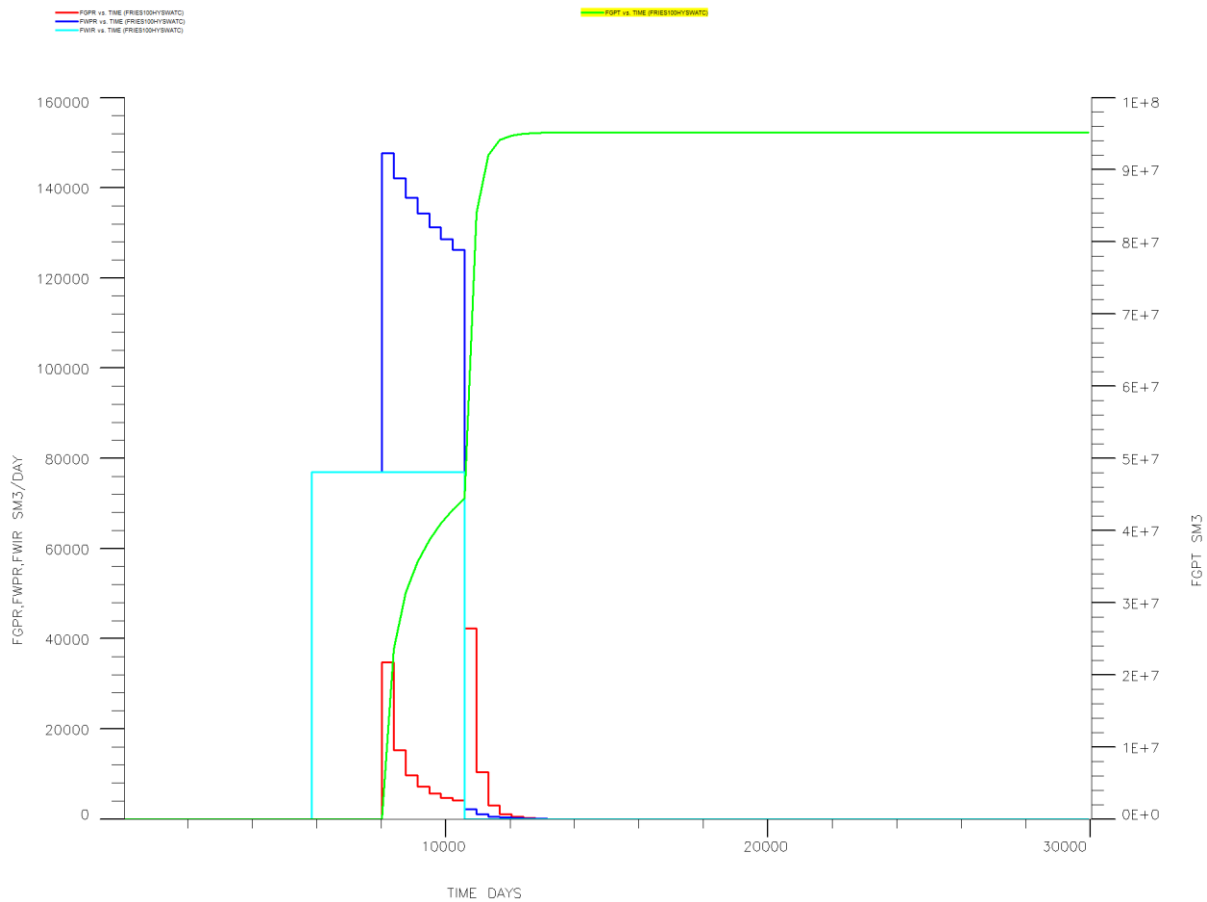


Figure 18. Leakage rates (red) as a function of time in a situation where the initial leak starts 6 years (2091 days) after the massive water production and injection (blue) has started. Furthermore this water production/injection continues another 7 years (scenario 4c).

The second peak in venting rates (Figure) can be avoided when the period of production/injection of water is extended to 4745 days or 13 years (Figure , scenario 4d). In this scenario, the emission of CO₂ stops together with the injection of brine. This can be attributed to the sudden drop in pressure at the site of the injector below the pressure constraint of the venting well.

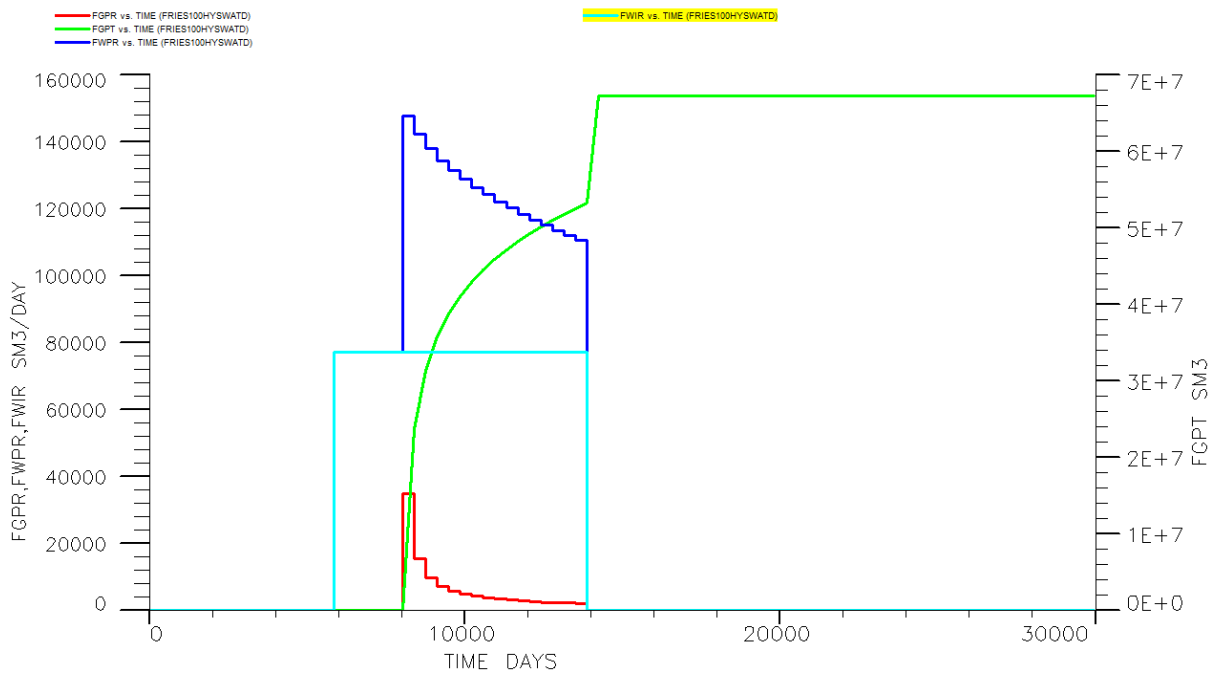


Figure 19. Venting rates (red) as a function of time in a situation where the initial leak starts 2190 days or 6 years after the massive water production and injection (blue) has started. Furthermore this production/injection of water continues another 4745 days (scenario 4d).

Table 3. Overview of the cumulative emission for the scenarios 4a, 4b, 4c 4d, 4e, 4f, 4g and 4h.

Scenario	Cumulative emission ($\cdot 10^7 \text{ Sm}^3$)	% of total injected CO ₂
4a	275	8.6
4b	8.85	0.28
4c	9.51	0.30
4d	6.77	0.21
4f	3.95	0.17
4g	0.658	0.057
4h	0.16	0.016

Comparing Table 2 and Table 3 reveals that water injection is far more efficient in reducing emission rates during venting than hysteresis by itself. The results in Table 3 also show that simultaneous water injection with the venting is more efficient as water injection prior to the venting procedure. That indicates that injection of water to displace the CO₂ from the venting injector is more efficient than relying on immobilizing the CO₂ phase by capillary entrapment (part of the hysteresis process).

5 CONCLUSIONS

Although hysteresis and the associated entrapment of CO₂ somewhat suppresses the amount of emitted CO₂ during unintended flow of CO₂ towards the surface, they generally cannot stop the unwanted flow of CO₂ from large injection sites. The amount of vented CO₂ decreases with the time-span between the end of CO₂ injection and opening of the injector. This is due to the migration and spreading of CO₂ within the aquifer. This spreading means that more CO₂ is captured by the brine imbibition after the well is opened and it is also more likely that this imbibing process may disconnect the otherwise continuous CO₂ phase

The relative permeability's during the imbibition cycle were estimated using a software algorithm. Using actual measured hysteretic relative permeability's may lead to more or less favorable results of emissions during venting as the actual entrapment of CO₂ may be affected. It should also be noted that hysteresis is a natural process, and that non-hysteretic conditions only occur within reservoir models. The results show that the venting emissions are overestimated when the hysteresis process is ignored.

Results of back production should be independent of the size of the aquifer, as the volume of the compressed water is far greater than the volume of CO₂. The permeability did not have a large effect on the amount of back production. The amount of injected CO₂ was by far the most important parameter in determining the amount of back productions.

With hysteresis being a natural process and the limited impact of permeability, pore-volume (all within the range seen in actual aquifer storage projects) on the predicted emission rates during venting, the only remaining key factor is the amount of injected CO₂.

It is also complicated to stop the back production of CO₂ in an opened well by the injection of brine at the same reservoir location, but emission rates of CO₂ can be strongly reduced. Again the fraction of stored CO₂, which is emitted, depends on the amount of CO₂ stored. At low values for the stored CO₂, simultaneous injection of water at the site of the venting came very close (less than 1 % of the stored CO₂) to a complete elimination of the unwanted CO₂ flow.

It should be noted that this report deals with rather extreme leakage scenarios including the very large potential flow caused by a completely opened injector in combination with an aquifer in which a massive amount of CO₂ was injected (for comparison 5 times as much as currently in the Sleipner field).

Although the injection of up to $3.65 \cdot 10^5$ m³ of brine was unable to entrap all this CO₂. The process of diverting the CO₂ away from the injector was far more efficient in eliminating the CO₂ emissions during the venting procedure.

Combining venting and water injection as a corrective measurement may therefore be useful in situations where reducing the reservoir pressure is required but significant venting rates should be avoided. Examples could be urban settings. Injection of water to displace the CO₂ away from potential leak may also be useful. When CO₂ is leaking through a faulty injector, the water injection near the perforations will also reduce the emissions.

6 REFERENCES

- Benson, S.M. Pini, R., Reynolds, S.V.C., Niu, B., Calvo, R. and Niemi, A. (2015). Relative permeability for multiphase flow in CO₂ storage reservoirs. Part II Resolving fundamental issues and filling data gaps. Global CCS Institute Report (GLOBALCCSINSTITUTE.COM).
- Corey, A.T. (1994). Mechanics of immiscible fluids in porous media. Water Resources Publications, Highlands Ranch, CO, USA, 252 pp.
- Doughty, C. (2007) Modeling geologic storage of carbon dioxide: Comparison of non-hysteretic and hysteretic characteristic curves.48: 1768–1781
- Esposito, A. and S.M. Benson (2012). Evaluation and development of options for remediation of CO₂ leakage into groundwater aquifers from geologic carbon storage. International Journal of Greenhouse Gas Control 7 (2012) 62–73
- Hovarka, S.D. (2006). Frio brine storage experiment –lessons learned. GCCC Digital Publication Series #06-13.
- Lenhard, R.J and Parker, J.C (1987) A model for hysteretic constitutive relations governing multiphase flow: 2. Permeability-saturation relations. Water Resources research 23; 2197-2206.
- Neele, F., Nepvue, M., Hofstee, C., and W. Meidertsma (2011). CO₂ storage capacity assessment methodology. TNO-report: TNO-060-UT-2011-00810
- Oak, M.J. (1990). Three-phase relative permeability of water-wet Berea. In: Seventh Symposium on Enhanced Oil Recovery, Paper SPE/Doe 20183. Tulsa, OK, April 22-25
- Parker, J.C and Lenhard, R.J. (1987). A model for hysteretic constitutive relations governing multiphase flow: 1. saturations-pressures relations. Water Resources Research 23; 2187-2196.
- Juanes, R., E. J. Spiteri, F. M. Orr Jr., and M. J. Blunt (2006). Impact of relative permeability hysteresis on geological CO₂ storage, Water Resour. Res., 42, W12418, doi:10.1029/2005WR004806.

APPENDIX 1

In this appendix, several additional simulations will be discussed, such as a sensitivity analysis of the venting procedure as described in Chapter 3.

The first simulation concerns a reduction of the pore volume in half the aquifer (around the injector) by a factor 0.5. To compensate for this reduction, the pore volume in the rest of the aquifer was multiplied by a factor 2, so that the total pore volume of the aquifer remained the same. This is to avoid any issues with the reservoir pressure. Figure A.1 shows that the back production is still high and close to the earlier hysteretic models.

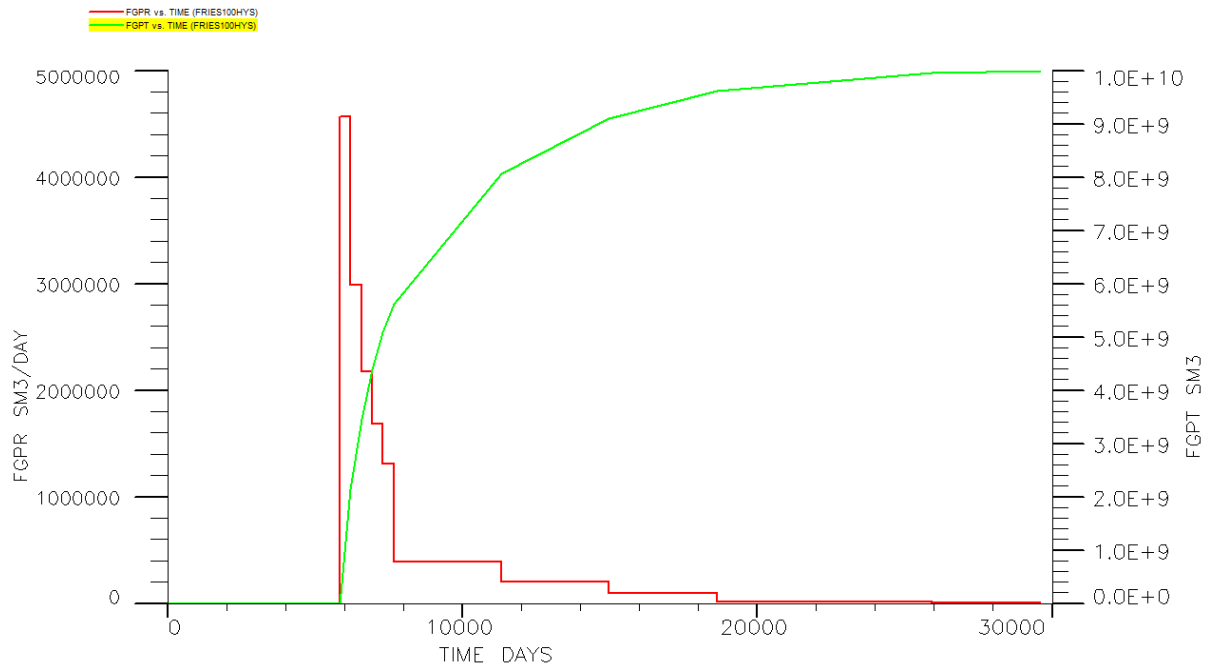


Figure A.1. The back-production rate and cumulative production for a simulation with pore volume multiplier of 0.5 around the injector.

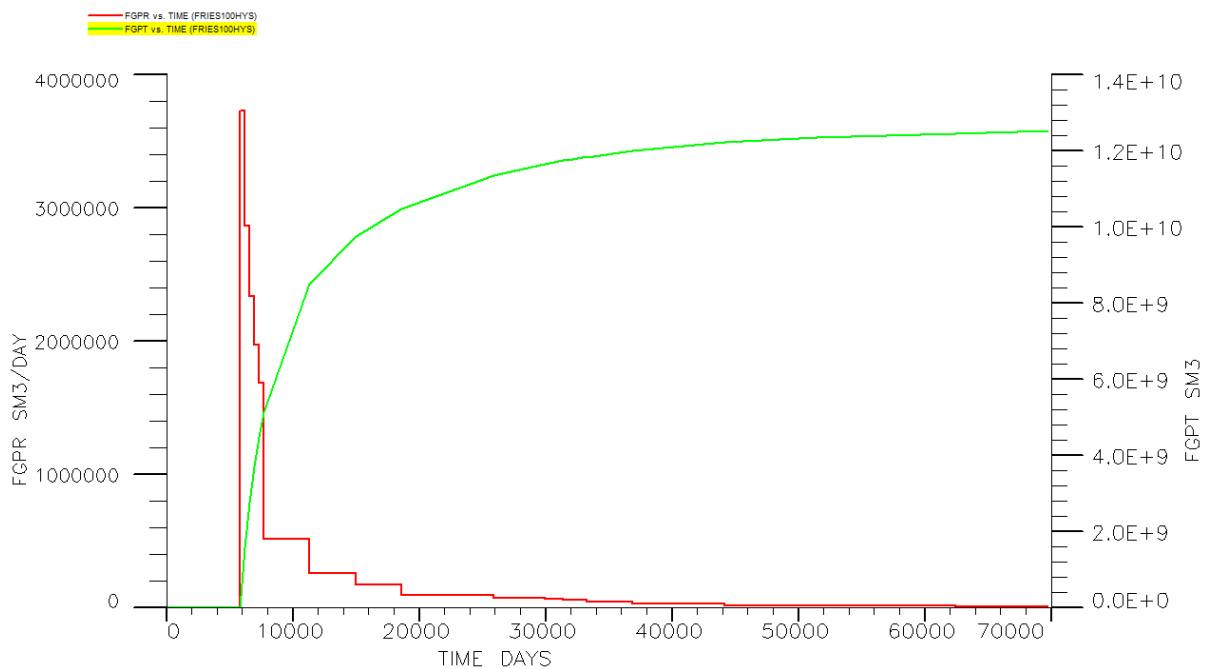


Figure A.2. The back-production rate and cumulative production for a simulation with permx multiplier of 4 on the horizontal permeability.

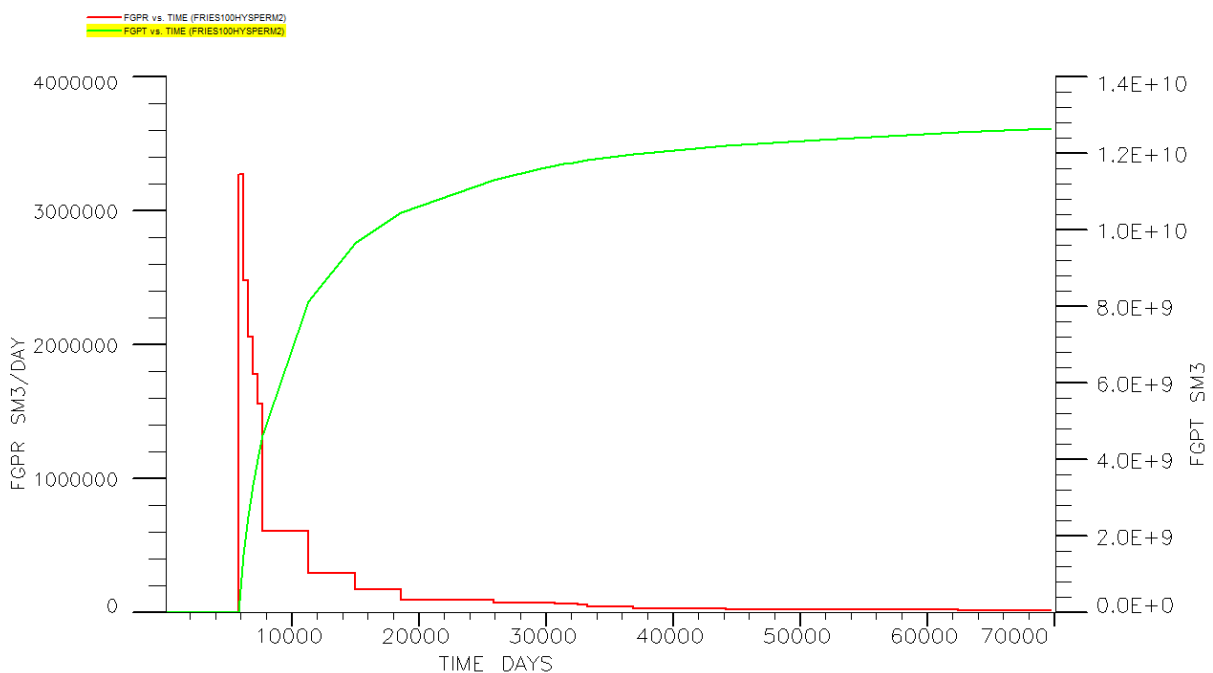


Figure A.3. As Fig. A.2, but with a global multiplier of 0.5 on the horizontal permeability .

Although, as expected, the initial back production rates are higher for the high permeability than the low permeability, the cumulative back production quantities are very similar.

In the following scenarios, an analysis will be conducted in which the quantity of CO₂ injection is systematically reduced (the following prediction using half the previous amount, until the back production stops).

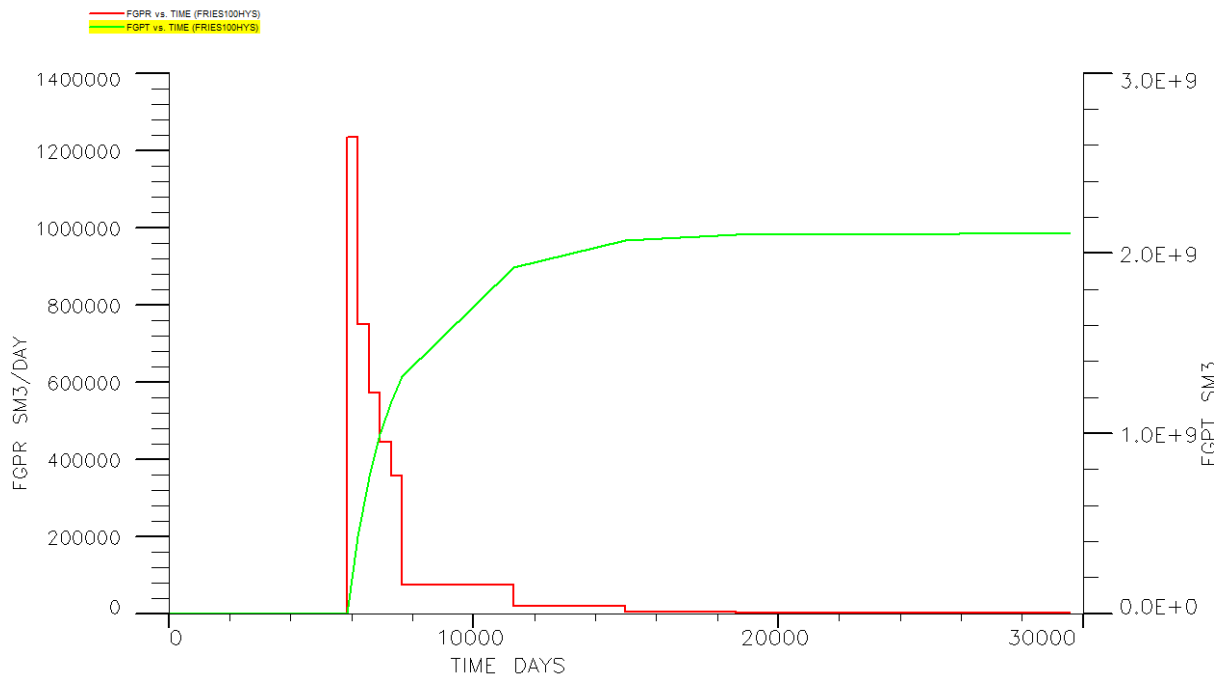


Figure A.4. Venting rates and cumulative back production after an injection of $16 \cdot 10^9 \text{ Sm}^3$ of CO₂ (half than that in Chapter 3).

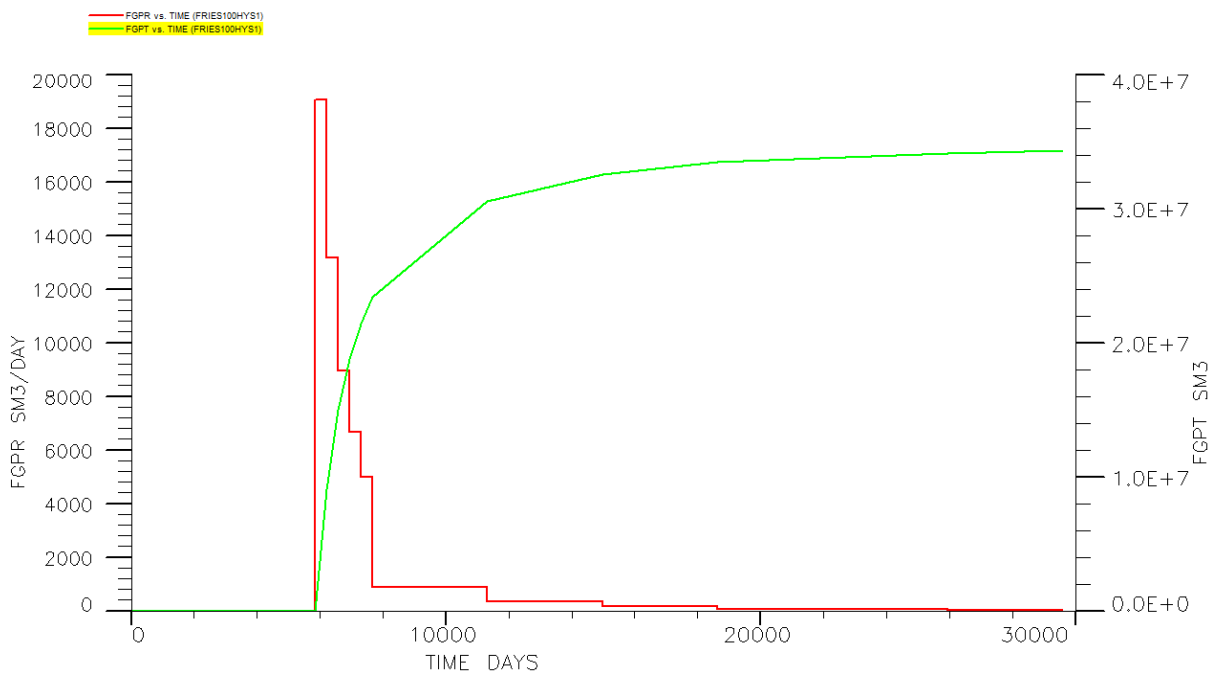


Figure A.5. As Fig A.4, but after $8 \cdot 10^9 \text{ Sm}^3$ Mton of CO₂ injection.

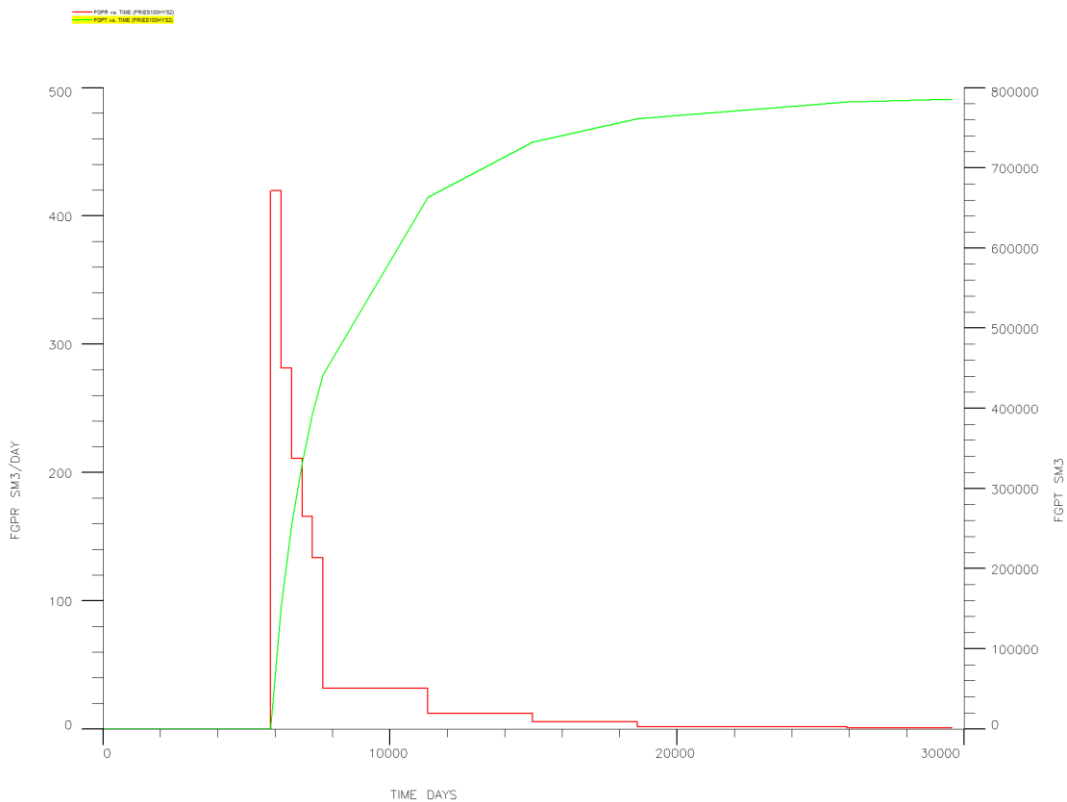


Figure A.6. As previous figure, but with half the cumulative injection (410^9 Sm^3).

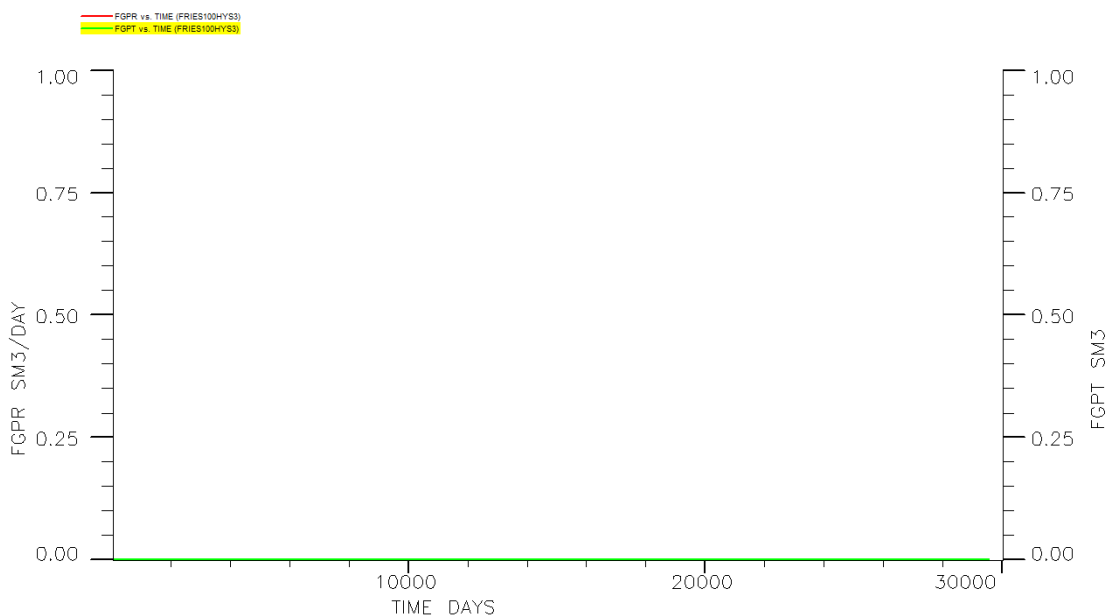


Figure A.7. As previous Figure, but with $2 \cdot 10^9 \text{ Sm}^3$ injection.

After $2 \cdot 10^9 \text{ Sm}^3$ of injection, no back production was predicted (Figure A.7). Further reduction of the injection was therefore not conducted. The results of all scenarios in this Appendix are summarized in Table 2.